



# The effect of trepanning speed of laser drilled acute angled cooling holes on the high temperature low cycle corrosion fatigue performance of CMSX-4 at 850 °C



N. Morar<sup>a</sup>, R. Roy<sup>a</sup>, J. Mehnen<sup>a</sup>, J.R. Nicholls<sup>b</sup>, S. Gray<sup>b,\*</sup>

<sup>a</sup>The EPSRC in Through-life Engineering Services, Cranfield University, MK43 0AL, UK

<sup>b</sup>Surface Engineering and Nanotechnology Institute, Cranfield University, MK43 0AL, UK

## ARTICLE INFO

### Article history:

Received 8 December 2016

Received in revised form 28 April 2017

Accepted 28 April 2017

Available online 4 May 2017

### Keywords:

Hot corrosion

Low cycle fatigue

Corrosion fatigue

Laser drilling

Recast layer

CMSX-4

## ABSTRACT

The effect of laser trepanning speed and, as a result, recast layer thickness on the high temperature corrosion fatigue behaviour of CMSX-4 superalloy acute angled holes was investigated. The experimental test results show that an increasing laser drilling speed caused a reduction in corrosion fatigue life by 35–50% at 850 °C, under low cycle fatigue regime. This reduction was found to correlate directly with the recast layer thickness and surface anomalies within the recast layer produced during the laser drilling process. Corrosion had a smaller effect on the overall life of the laser drilled specimens under the conditions tested. The results presented show that laser trepanning speed is influential in limiting the life performance of laser drilled components in service.

© 2017 The Authors. Published by Elsevier Ltd. This is an open access article under the CC BY license (<http://creativecommons.org/licenses/by/4.0/>).

## 1. Introduction

One of the main applications of the laser drilling process in the aerospace industry includes the manufacture of cooling holes in hot section turbine blades, nozzle guide vanes and combustor liners. These components are usually made of nickel-base alloys that are resistant to high temperature and associated corrosion environment. However, the laser drilling process is known to produce localised stress concentrations, a recast layer and associated microstructural and mechanical properties changes due to these surface breaking holes [1]. Therefore, the potential for degrading the alloy corrosion resistance and increasing the susceptibility to hot cracking [2]. The severity of the surface damage due to laser drilling is dependent on the laser intensity, which, in turn, depends on the laser trepanning/percussion parameters used. Previous studies have shown that for the Nd:YAG laser drilling process, parameters such as pulse energy, pulse duration, pulse frequency, and drilling speed are the most influential; increasing the recast layer thickness and leading to micro crack formation both in percussion [3] and trepanning mode [4].

The effects of laser drilling processing on the fatigue strength of nickel-base alloys has recently been studied, showing the effects of

roundness error on the cooling film holes through experimental and finite element (FE) modelling [5]. The results showed that irregularities on the contour profile of the laser drilled hole caused by the recast layers could significantly decrease the life of the drilled holes. Moreover, the larger the roundness error, the shorter the low cycle fatigue life. In another study, Degeilh et al. [6] investigated laser drilling effects on three different hole diameters. A damage model was used to characterise the fatigue lifetime. The model consisted of a 3D averaging method that takes into account the material microstructure and hole shape. The results showed that small hole diameters, under 0.4 mm, had a better performance when compared to large hole diameters, under 0.8 mm, and electro-discharge machined (EDM) holes of diameters of between 1.0 and 2.0 mm. The difference between the laser and EDM drilling fatigue life was caused by the difference in the microstructure, thickness of the heat affected zone and surface roughness of the specimens.

Further studies have been conducted to assess the thermal-mechanical properties of thin-walled cylindrical specimens with laser drilled holes [7]. The results showed that the lives of laser drilled holes were four times shorter than that observed for smooth plain specimens under similar loading conditions. Pan et al. [8] used a local stress approach for assessing the fatigue life of laser drilled holes at high temperatures, between 700 °C and 900 °C. The metallographic analysis suggested that the microcracks

\* Corresponding author.

E-mail address: [S.Gray@Cranfield.ac.uk](mailto:S.Gray@Cranfield.ac.uk) (S. Gray).

induced by laser drilling had no significant influence on the total life of the specimen under a low cycle fatigue regime ( $10^5$  cycles). In an earlier study, Gemma and Phillips [9] used fracture mechanics to predict the life of different cooling hole configurations formed by laser drilling, EDM, and electrochemical machining (ECM) under thermal-mechanical fatigue conditions. They found that the defects introduced by the different drilling techniques generates a range of initial defect sizes and that this knowledge could be used to estimate the life of cooling holes for each drilling technique. Nevertheless, studies reported in current literature as above referenced have not fully detailed the laser drilling conditions and their influence on the corrosion fatigue behaviour.

This paper attempts to fill this gap in the literature, relating to the effects of recast layer thickness, varied by laser trepanning speed, on the high temperature low cycle corrosion fatigue (HT LCCF) life of CMSX-4<sup>\*</sup> nickel-based superalloy acute angled holes.

## 2. Experimental details

### 2.1. Specimen manufacture

The CMSX-4 material used for this study was in the form of single crystal cylindrical bars of 9.0 mm diameter that had been solution treated and aged. The chemical composition is listed in Table 1. The laser drilling was performed at an angle of 30 degrees on the fatigue specimens by a computer numerical control (CNC) Nd:YAG laser drilling machine. Due to the size and scope of this study, a decision was made to investigate only the laser trepanning speed settings. The decision was based on the reported work [4] and preliminary trial results conducted in previous work [10]. The three different laser trepanning speed settings selected has been shown to influence the recast layer thickness (RLT) and overall surface integrity of angled drilled holes. The remaining process parameters, including pulse energy, pulse duration, pulse frequency, nozzle displacement, focal point, and assisted gas pressure were kept constant for simplicity.

The laser drilling parameters employed based on parametric study [10], has ensured that the recast layer thickness after laser trepanning drilling (LTD) conditions A, B, and C achieved a range of values of between 4 and 85  $\mu\text{m}$  mean maximum values, see Table 2. It was not possible to measure the RLT of the pre-tested fatigue specimens and thus the data was obtained from CMSX-4 flat plate using the same drilling parameters as the fatigue specimens.

Post drilling processes including, ultrasonic cleaning, grit blasting, and heat-treatment were conducted according to the manufacturer standard procedures as this would reflect the current practices in the production of holes in hot section aircraft engine components. The details of the post-drilling processes are proprietary data. A total of 5 groups of specimens were investigated. Three were from laser drilled batches, one from EDM drilling, condition D (see Table 2), and lastly, an undrilled plain specimen group. Each fatigue specimen contained three angled holes at 30 degrees to the surface on a centre line, with a diameter of 0.75 mm, and a depth of 4.0 mm, as shown in Fig. 1. The spacing between drilled holes is similar to that found on the of hot section aircraft engine components.

### 2.2. Test procedures

A servo-hydraulic environmental fatigue testing machine was used to perform corrosion-fatigue testing at 850 °C, with a continuous flow of premixed air + 300 vppm  $\text{SO}_2$ , at a flow of 80  $\text{cm}^3/\text{min}$ .

Before testing, all specimens were coated around the gauge length with salt solution consisting of a fully saturated 98%  $\text{Na}_2\text{SO}_4$  + 2% NaCl mixture. This salt coating procedure, along with the test gas used, enables a good simulation, to achieve microstructures similar to those seen in the service operating environment of hot section aircraft engine components. The tests were conducted in a low cycle fatigue regime under load control to a stress ratio of zero and trapezoidal waveform of 1-1-1-1 s (0.25 Hz). Load control was used since strain control was not possible due to the test environment, and its containment, not being conducive for suitable strain measurement. The tests were performed at several maximal stress levels from as low as 290 MPa–550 MPa. The cyclic loading was applied continuously to each specimen until rupture occurred or a history of 110,000–120,000 cycles had been applied, at which point the testing was stopped and considered to be a run-out.

### 2.3. Metallography

After testing, all failed specimens were inspected via scanning electron microscopy (SEM) in order to confirm the fracture morphology and extent of corrosion. Electron dispersive X-ray spectroscopy (EDX) was used to identify the corrosion compounds on the fracture surface. Further examination required the fractured specimens to be cross-sectioned for measurement of the actual recast layer thicknesses. The metallographic preparation procedure is similar to that described in [10], with particular attention made to sectioning, grinding and polishing with an oil-base lubricant in order to minimise the loss of any corrosion products. The recast layer thickness measurements for the majority of the specimens were taken and recorded. These measurements were conducted at eight equally spaced points both from the leading edge side and trailing edge side of the hole. Only the maximum averaged values were used for the comparison and explanation of the results.

## 3. Results

### 3.1. HT LCCF tests

Fig. 2 shows the results of the tests conducted on the laser drilled specimens. Five sets of experimental data include laser drilling conditions: LTD set A (blue circle); LTD set B (green square), LTD set C (red triangle), and EDM (yellow diamond). The trend-line for non-drilled specimens is depicted as a black dotted line and has been tested under the same environmental conditions. As a comparison, unpublished air only data has been included that was supplied by the sponsor of this work using the same loading conditions. It can be seen, from a comparison of non-drilled corrosion data with the non-drilled air only data, that there is a debit of approximately 10% associated with the corrosion-fatigue interaction. However, when comparing the drilled holes with the air data, there is a performance debit of approximately 35%–50% (or 25%–40% assuming a cumulative effect) suggesting a much greater impact of the drilling process. The results also show that the HT LCCF behaviour of specimens with laser drilled holes at different conditions are dependent on the trepanned recast layer thickness. The poorest HT LCCF performance was obtained in laser drilling conditions A and C specimens which had the thickest estimated recast layer. The results confirm that the HT LCCF strength was strongly influenced by high trepanning speed. Moreover, it highlights that the recast layer thickness induced by the laser drilling process, when less than 50  $\mu\text{m}$  has the better fatigue life characteristics.

Further, unbroken specimens (previously stopped as a run-out) were later re-tested at an increased load in order to verify the endurance limit. The specimens with LTD set B conditions did

<sup>\*</sup> CMSX-4 is a registered trademark of Cannon-Muskegon Corporation.

**Table 1**  
The chemical composition of CMSX-4 superalloy (in wt%) [11].

Cr	Co	W	Re	Mo	Al	Ti	Ta	Hf	Ni
6.5	9.6	6.4	3.0	0.6	5.6	1.0	6.5	0.1	Bal.

**Table 2**  
Summary of laser trepanning drilling conditions and measured recast layer thickness on CMSX-4 plate.

Drilling conditions	Post-processing	Recast layer thickness
Laser Trepan Drilling Set A, Trepan speed at 125 mm/ min	Ultrasonic cleaning, Bead blast, heat treatment	Between 55 and 70 $\mu\text{m}$
Laser Trepan Drilling Set B, Trepan speed at 75 mm/ min	Ultrasonic cleaning, Bead blast, heat treatment	Less than 50 $\mu\text{m}$
Laser Trepan Drilling Set C, Trepan speed at 150 mm/ min	Ultrasonic cleaning, Bead blast, heat treatment	Greater than 75 $\mu\text{m}$
Die-sink EDM, Set D Pulse on-time (7 s)	Ultrasonic cleaning, Bead blast, heat treatment	Less than 25 $\mu\text{m}$
Pulse off-time (4 s) Pulse current (0.5 A) Dielectric fluid (Kerosene)		

not fail. The re-test at 400 MPa and 350 MPa strongly suggests an endurance limit closer to 400 MPa–350 MPa, which is about 100 MPa higher than the counterpart LTD set A and C conditions, re-tested at 290 MPa. Nevertheless, more tests are required to confirm these trends.

### 3.2. Recast layer thickness

Recast layer thickness (RLT) measurements were performed in order to confirm that for the down selected laser drilling conditions, obtained values are close to the estimated average of maximum RLT. The fractured fatigue specimens were examined by metallography, in which, specimens of each of the three sets were sectioned perpendicular to the axes of the holes and ground back

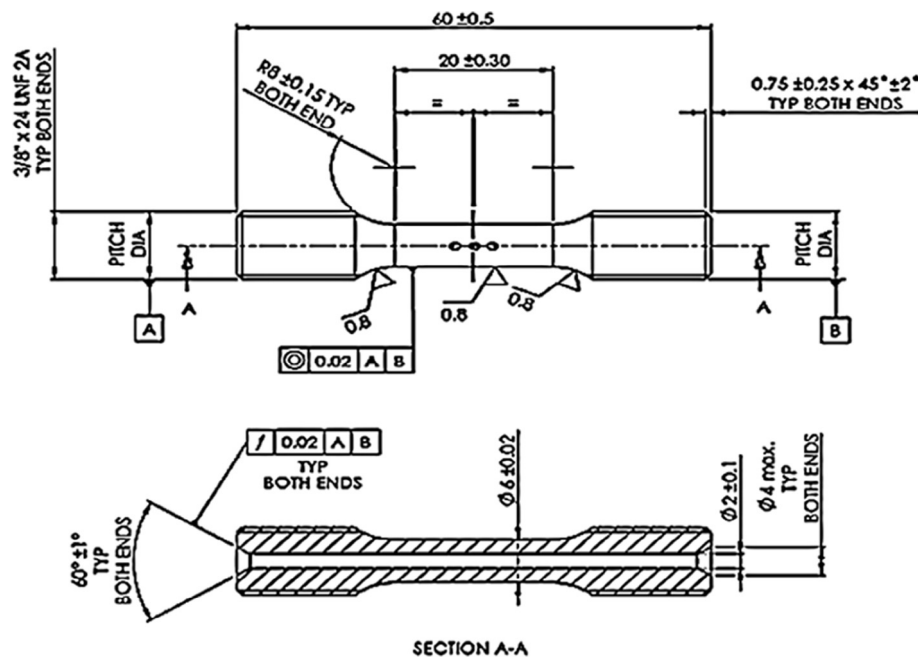
such as that the plane section was midway through the test piece. Measurements were made using an optical microscope and measuring points taken across the sectioned hole as described in Section 2.3. These measurements confirmed that the average maximum values of RLT were under the estimated boundaries, as presented in Table 3.

Fig. 3a–d shows examples of cross-sections of selected fatigue specimens. It can be seen from the SEM micrographs how the recast layer thickness is influenced by the different trepanning speeds, in that a higher trepanning speed results in a thicker recast layer. Fig. 4 also demonstrates that cracks in the recast layer after processing may act as preferential initiation sites for fatigue cracking.

### 3.3. Metallography examination of fractured specimens

Fractured surfaces of all failed specimens were examined using an SEM in order to observe whether the recast layers could have acted as a driver for the crack initiation in the laser drilled holes. It was found that the main fatigue crack initiated from the recast surface layer both at the upper right and left acute corner of the hole edges, as highlighted with yellow squares in Fig. 5. These sites of crack initiation are regions of high stress concentration around the elliptical holes as per [12,13]. Cracks then propagated into the substrate perpendicular to the direction of the applied load until the final fracture. Multiple cracks were also observed in other regions of the surface breaking hole, where the stress concentration is somewhat lower (see Fig. 6).

Fig. 6a–d illustrates an example of an unbroken specimen where cracks were formed in the vicinity of the specimen surface breaking hole. It can be seen in Fig. 6, that there are cracks within and outside of the recast layer boundary. These are also similar to the cracks observed at the remaining holes which did not fractured



**Fig. 1.** Dimensional specification of fatigue specimens with laser drilled holes. All dimensions are in mm.

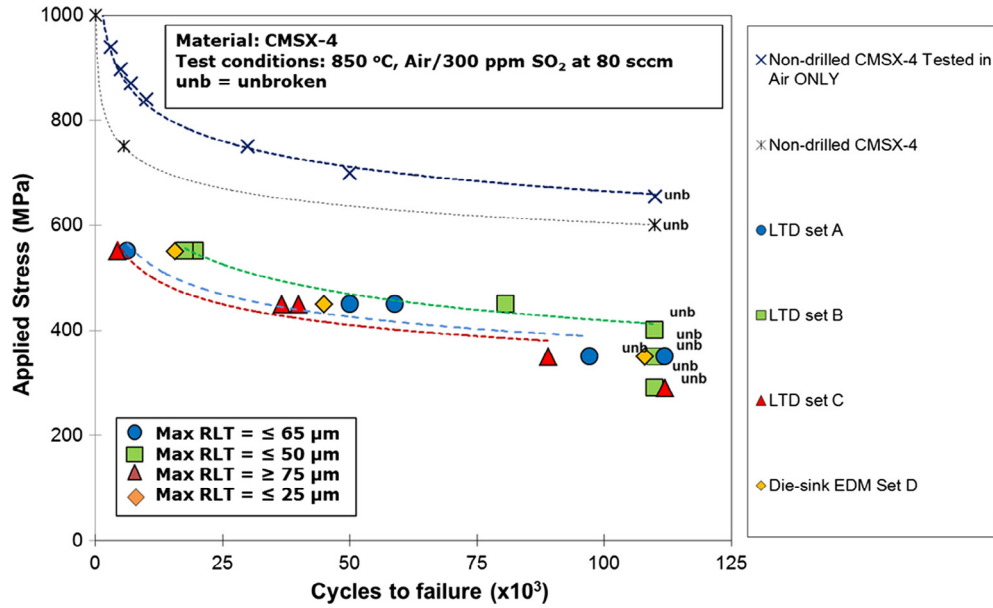


Fig. 2. S-N curves of HT LCCF life of laser drilled specimens with different processing settings. Power law fits have been included for each data set.

Table 3  
Summary of the recast layer thickness (RLT) measurements.

Drilling method	Post fatigue test mean RLT	Pre-test RLT
LTD set A	62 $\mu\text{m}$	Between 55 $\mu\text{m}$ and 70 $\mu\text{m}$
LTD set B	48 $\mu\text{m}$	Less than 50 $\mu\text{m}$
LTD set C	78 $\mu\text{m}$	Greater than 75 $\mu\text{m}$
Die-sink EDM set D	22 $\mu\text{m}$	Less than 25 $\mu\text{m}$

from failed fatigue specimens. This indicates that the majority of the cracks could have been formed during the cyclic stressing of the specimen from the brittle recast layer. The severity of the crack extension is expected to depend on the high stress concentration and propagate from the region of highest stress.

Examples of fracture surfaces of two failed specimens tested at high stress and low stress level are shown in Fig. 7a–d. In both

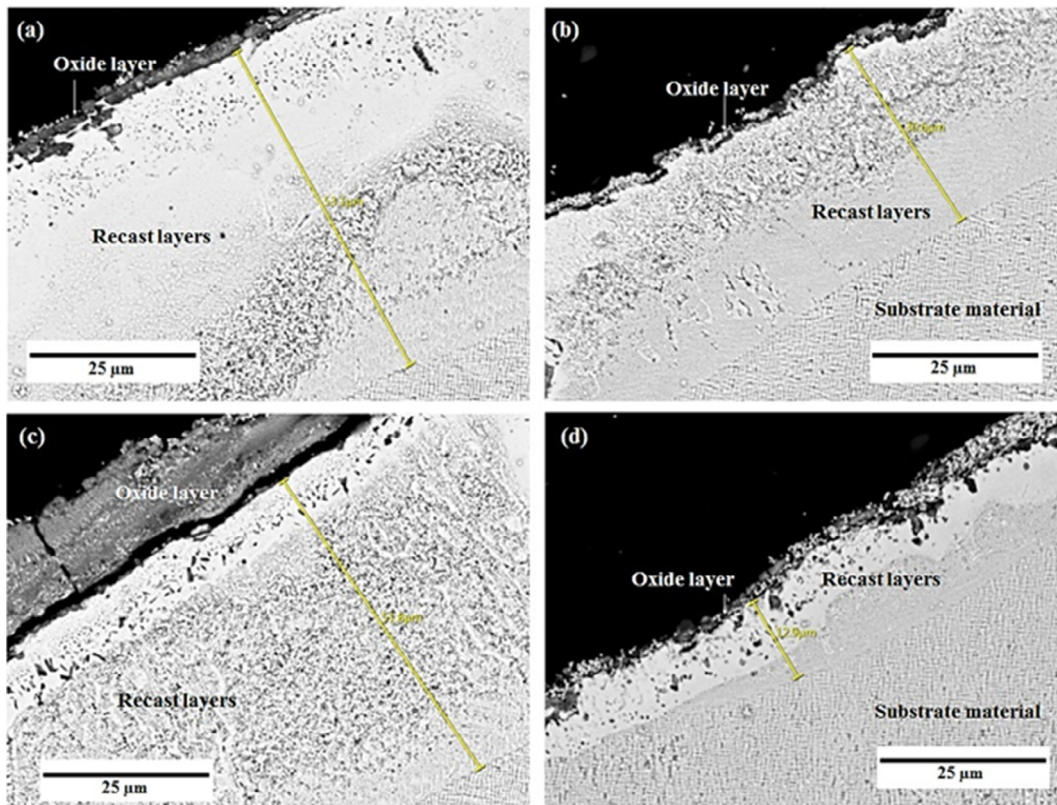


Fig. 3. Examples of SEM micrographs showing the recast layer morphology under different drilling conditions tested: (a) LTD set A; (b) LTD set B; (c) LTD set C; and (d) Die-Sink EDM set D.

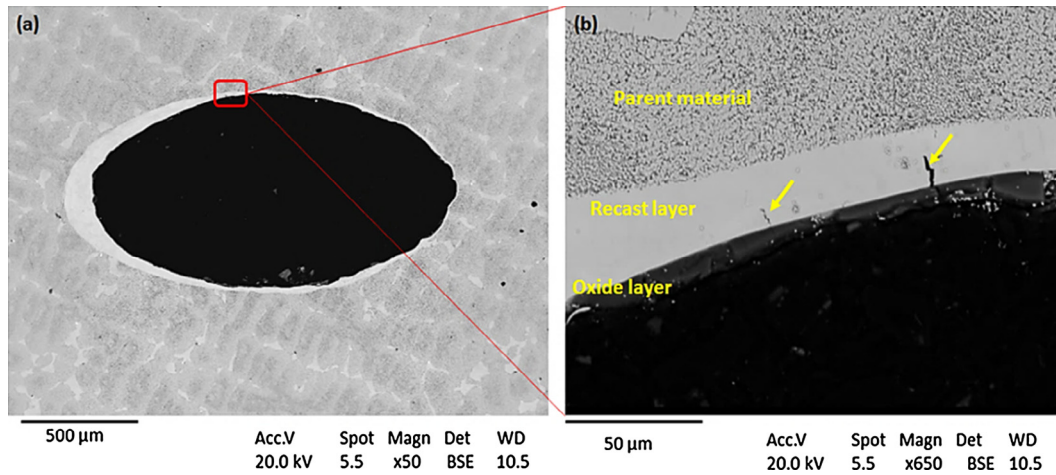


Fig. 4. Backscatter micrographs shows an example of microcracks observed on the top surface of a LTD set A sample after drilling.

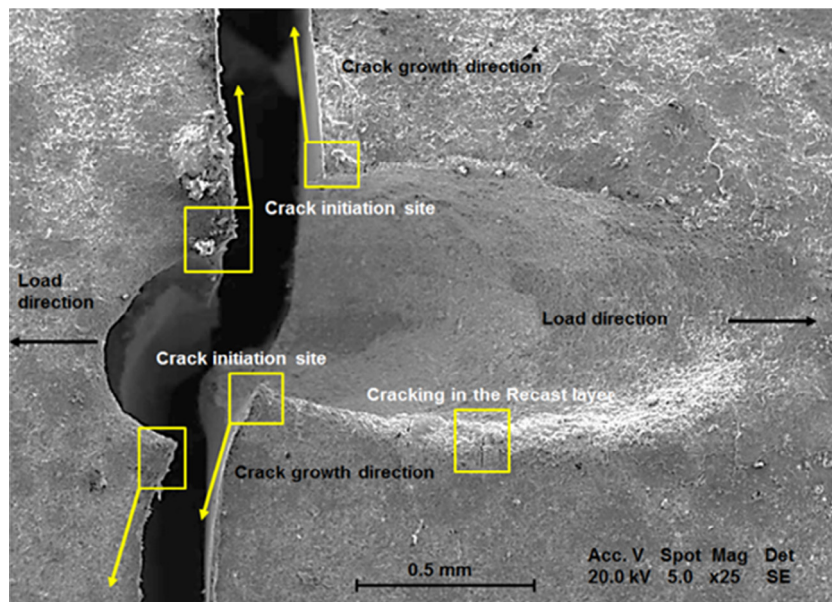


Fig. 5. SEM micrograph of a fracture fatigued specimen showing an example of observed crack initiation sites and crack growth direction in laser drilled acute elliptical holes.

cases, fatigue cracks are expected to initiate within the recast layer, extending in the form of thumbnails, with crack growth facets consistent with cleavage fracture and tensile dominated fracture mode towards final fracture. At high cyclic stress level, the final fracture was a mix of ductile and tensile overload, with evidence of rough fracture features including cleavages and slip bands (see Fig. 7a). Whereas, at low and intermediate cyclic stresses the final fracture occurred by ductile overload (see Fig. 7c and d).

Evidence of high temperature corrosion was observed in all specimens tested, but it was more prominent at lower cyclic stresses where specimens lasted longer before final fracture. The data points in the S-N curves generated at high stresses resulted in shorter lives and under 20,000 cycles, gives insufficient time for the corrosion mechanism to develop fully. At intermediate and lower stresses, specimens had longer lives but limited to 110,000 cycles when they removed from the test. Under these cyclic stresses, there is an evidence of corrosion on the specimen's surface but not enough to affect the overall observed fatigue life.

Fig. 8 shows an example of oxidation and sulphidation found for a specimen tested at low cyclic stress conditions. The micrograph

confirms the presence of mixed oxides and sulphidation process. The mixed oxides form a protective layer on the sample surface rich in nickel, aluminium, and chromium, forming an alumina ( $\text{Al}_2\text{O}_3$ ) and chromium sulphide ( $\text{Cr}_2\text{O}_3$ ) layers [14]. These layers protect the alloy surface from the hot corrosion mechanism. The sulphidation process is known to attack as soon as the alumina protective layer degrades and begins to cracking. It is degraded alumina layer facilitating the sulphur propagation below the protective layers, and in some cases through the crack tips. The crack tips allow diffusion of sulphur into the base alloy accelerating the corrosion and further degrading alloy properties, in particular the fatigue strength [15]. The cracking in the protective oxide layer occurs due to different thermal expansion coefficients of oxides, which also causes additional stresses. Overall, sulphidation process has shown to be relatively slow at crack growth stage compared to incubation (initiation) time under the low cycle fatigue regime. It appears that the absence of grain boundaries in CMSX-4 superalloy resisted the high temperature corrosion mechanism in the propagation stage, particular for specimens tested at 350–290 MPa. The surface morphology shown in Fig. 8 is consistent with a HT corrosion type I microstructure reported [16] for this specimen tested at 850 °C.

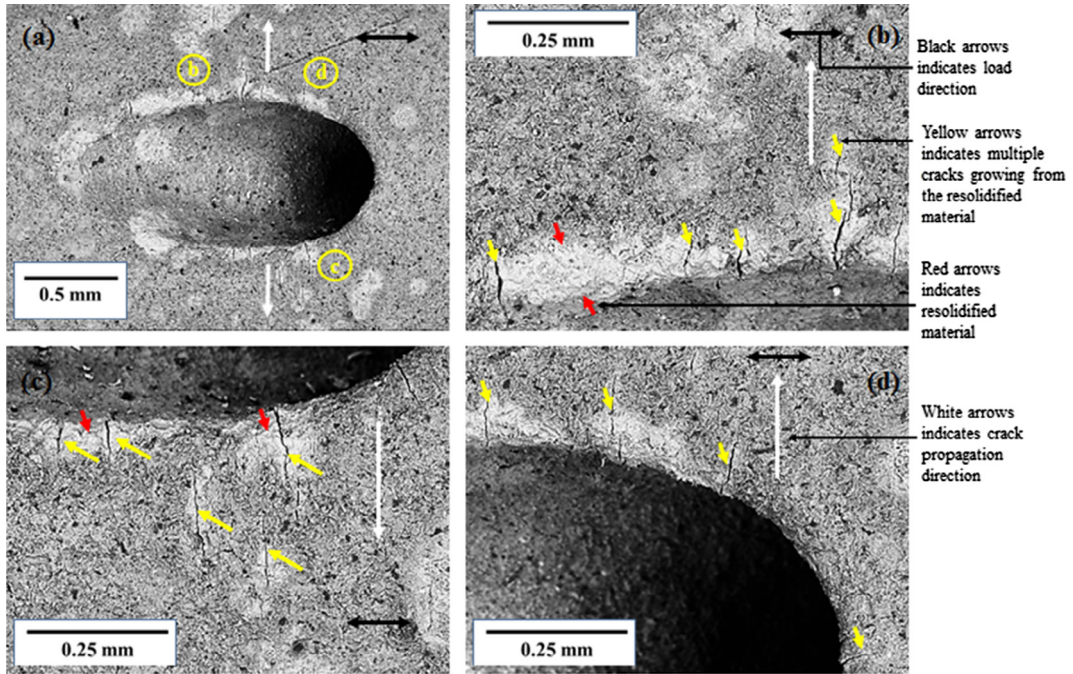


Fig. 6. Scanning electron microscopy images showing an example of multiple cracks observed on an unbroken specimen tested at 350 MPa.

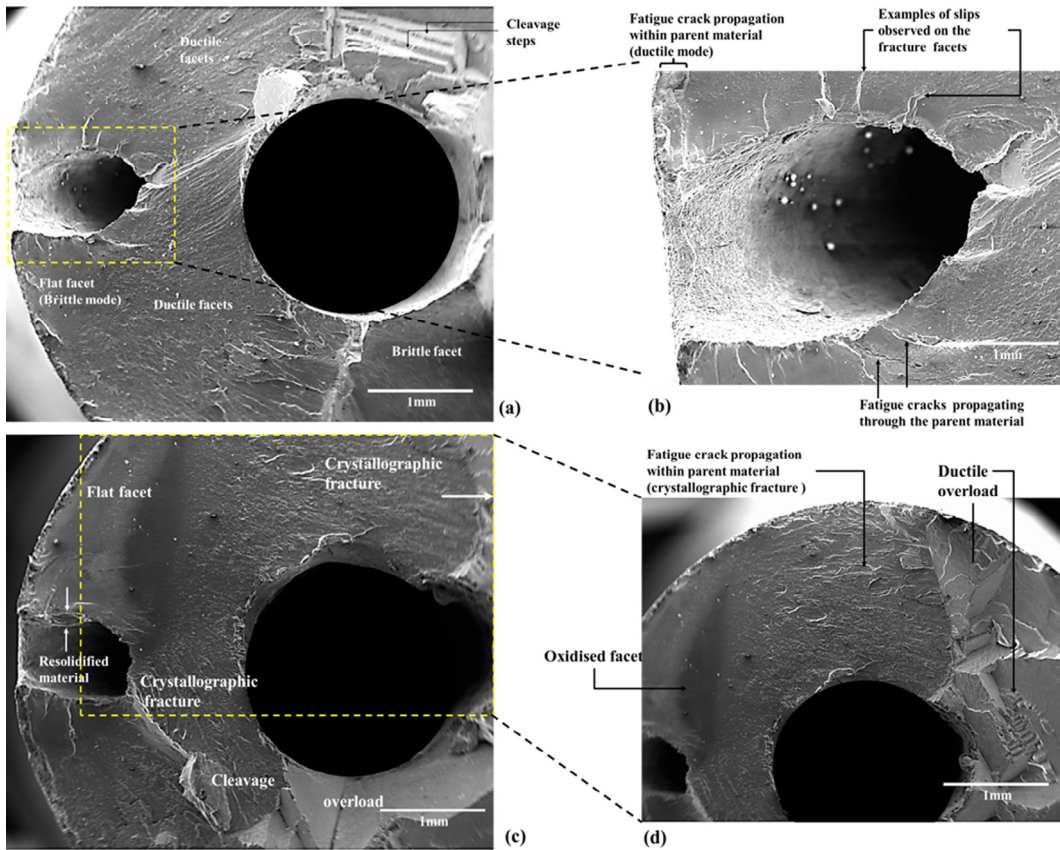
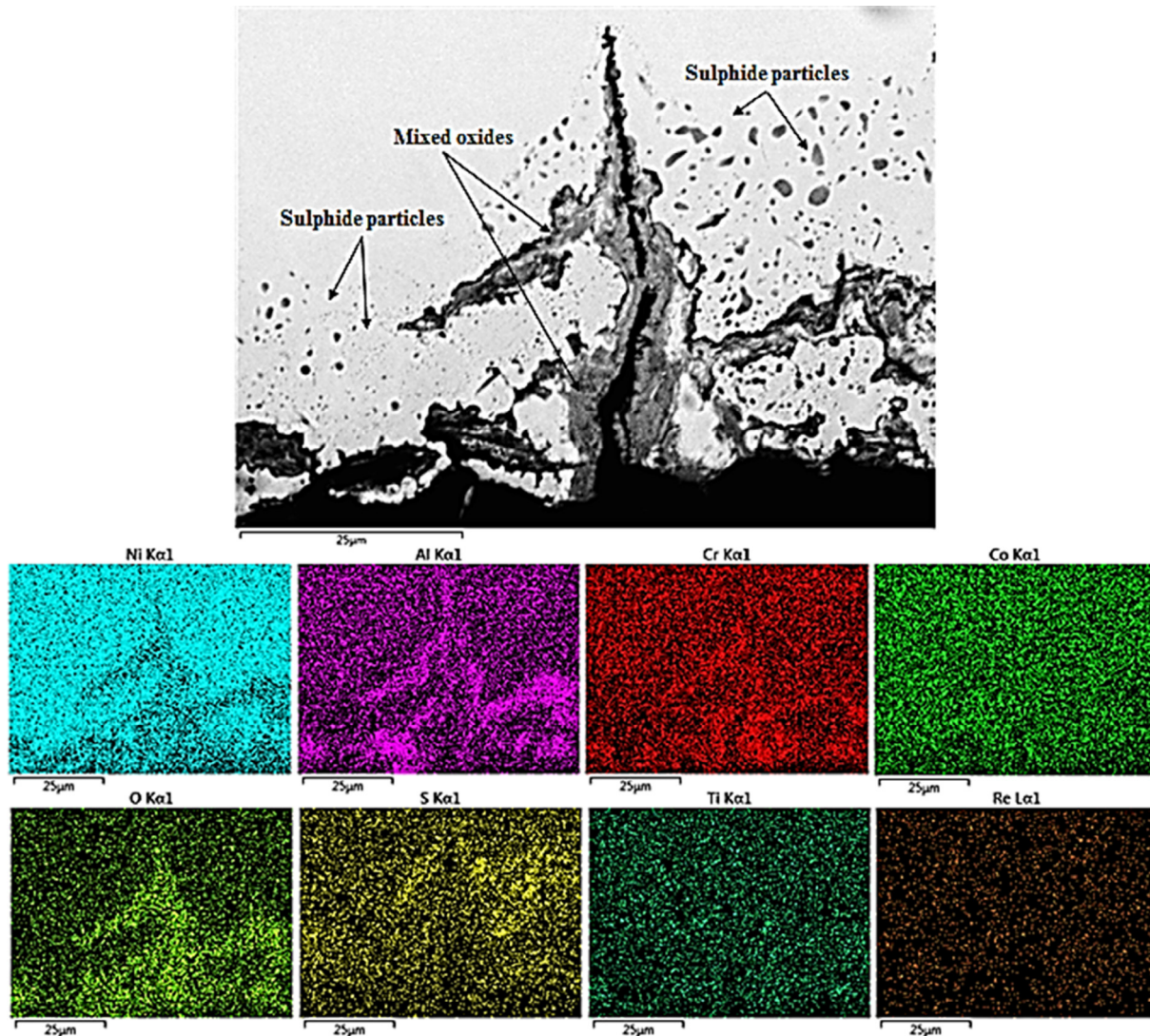


Fig. 7. SEM micrographs showing two examples of fracture surfaces on specimens: (a and b) tested at 550 MPa, LTD set A (FAT 233); and (c and d) specimens tested at 350 MPa, LTD set C (FAT250).



**Fig. 8.** Backscattered electron image of a typical sulphidation cracking found under a tested specimen (LTD set A). Also shown is the element mapping of main mixed oxides and sulphur compounds detected by the EDX analyser.

## 4. Discussion

### 4.1. Influence of laser drilling parameters on HT LCCF life

Examining the S-N data (Fig. 2), it is observed that in general, all laser drilled fatigue specimens have experienced a reduction in life compared to undrilled specimens. The HT LCCF response at higher stress levels was dominated by the effects of the high cyclic stress. Therefore, only a small variation in fatigue lives between each set of laser drilled specimen was observed. Variation in HT LCCF life was prominent at intermediate stress level (450 MPa) and at low stress levels (350 MPa–290 MPa). The S-N curves of the three laser drilled conditions suggests that the HT LCCF behaviour was dependent of the recast layer thicknesses obtained at each LTD parameter set for a given applied cyclic stress. The fractography and EDS analysis indicates that hot corrosion had minimal effect on the overall life of the specimens. This may be due to the specimens being exposed for a limited period of time thus not allowing for corrosion damage to fully establish. Or it could also be attributed to the dominant effect the recast layer has on the fatigue life, when pre-cracking is already presented (see Fig. 4).

Further, the S-N data was used to analyse the lives of laser drilled specimens at different peak power settings and comparing their lives with the Die-sink EDM specimens at the same stress level, as presented in Figs. 9a–b and 10a–b. It can be seen from these plots that the influence of trepanning speed on the HT LCCF life becomes more pronounced as the value of the trepanning speed increases. Although the number of EDM'ed specimens used for the comparison was very limited, the work shows a life that is similar for LTD set A and LTD set C specimens. The EDM'ed drilled specimens had a maximum mean RLT of 22 µm, from metallographic examination. This means that thick recast layers, whether induced by laser drilling or die-sink EDM drilling method have a detrimental impact on the fatigue strength. It is also true that in general EDM drilling induces an average recast layer thickness of 10–15 µm for holes with a diameter range of 0.5–1.0 mm [6]. Therefore, better fatigue life characteristics than the laser drilled specimens would be expected, additional tests are required to confirm this trend.

Comparing the data obtained at different laser trepanning conditions, the maximum recast layer thickness values ranged from 4 µm to 80 µm when the trepanning speed increased from a low

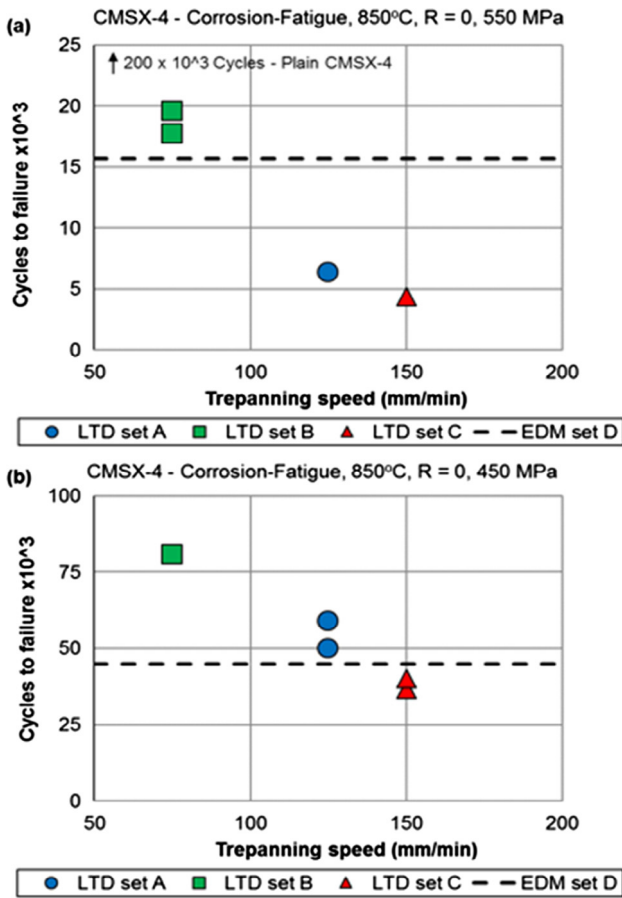


Fig. 9. Effect of trepanning speed on the hot corrosion fatigue life of CMSX-4 laser drilled acute and angled holes at (a) 550 MPa and (b) 450 MPa.

setting to higher setting. Trepanning speed seems to be the main process parameters affecting the fatigue life, and interestingly, overall best responses are obtained when the fatigue specimens are produced using LTD set B (low trepanning speed setting). This study establishes the correlation between trepanning speed, recast layer thickness and fatigue life. The endurance limit for both specimens with thin (LTD set B) and thick (LTD set A and LTD set C) recast layers is circa 350 MPa and 290 MPa, respectively. However, it is appreciated that more testing should be performed to fully validate these endurance limit values.

Moreover, it is known that the recast layer and micro-crack formation in laser drilled holes is dependent on process parameters [17,18]. It has also been shown in this study that increasing trepanning speed not only could lead to the formation of thick recast layers but also formation of micro-cracks. The surface crack length examined from previous work [10] shows that the severity of cracking in laser drilled holes is also associated with thick recast layers greater than 50  $\mu\text{m}$ , and the present investigation has shown this to give poor fatigue life. Fractography examinations also suggest that the surface crack initiation is easier from the brittle recast layers and any surface anomalies surrounding the laser drilled holes. Crack growth into the base material was mostly dependent on cyclic stress and severity of the corrosive species diffused into the crack tip, most likely gaseous S and  $\text{O}_2$ . From this understanding, surface crack initiation is strongly related to the recast layer induced by the laser drilling process and growth is dependent on mechanical load and environmental test conditions. Therefore, laser drilled holes with high surface quality are recommended. It is not unreasonable to think that smoother surfaces lead to lower local stress concentration and would allow fatigue lives to be extended

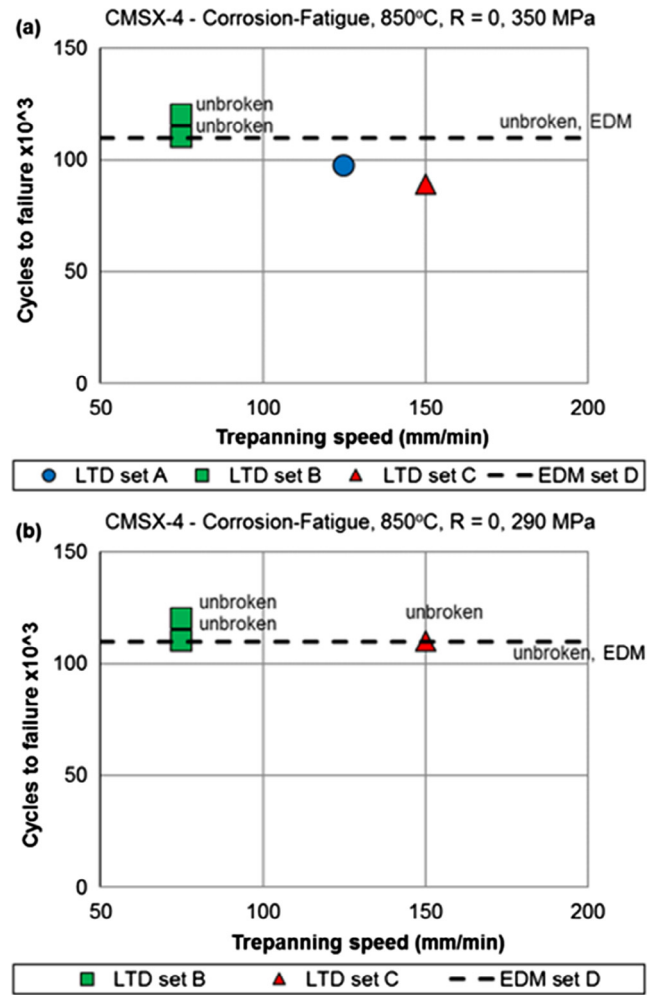


Fig. 10. Effect of trepanning speed on the hot corrosion-fatigue life of CMSX-4 laser drilled acute and angled holes at (a) 350 MPa and (b) 290 MPa.

### 5. Conclusions

The effect of laser trepanning drilling speed on the high temperature low cycle fatigue lives of CMSX-4 with acute angled holes at 850 °C were investigated. The key findings of this work are:

- Increasing the laser trepanning speed increased the recast layer thickness.
- Corrosion fatigue of undrilled CMSX-4 under the test conditions caused a performance debit of approximately 10% when compared to air data.
- Laser trepanned acute angled holes show a corrosion-fatigue performance debit of approximately 35%–50% when compared to undrilled air material. This debit was related to the recast layer thickness produced.
- Recast layer thickness was sensitive to trepanning speed and the best performing specimens, with approximately 35% performance debit, were obtained using the slowest trepanning speed of 75  $\text{mm min}^{-1}$  and possessed the thinnest recast layer.

### Acknowledgement

The authors are thankful to the Engineering and Physical Science Research Council for financial support of the research work (Grant number EP/I033246/1) and Rolls-Royce Plc for the technical



support and useful discussions. Data underlying this study can be accessed through the Cranfield University repository at <http://dx.doi.org/10.17862/cranfield.rd.4978220>. The authors would also like to acknowledge Dr Tracey Roberts at Cranfield University for assistance with metallography work.

## References

- [1] Beck T, Coating TA, Gmbh R. Laser drilling in gas turbine blades shaping of holes in ceramic and metallic coatings. *Laser Tech J* 2011;8:40–3.
- [2] Neidel A, Riesenbeck S, Ullrich T, Völker J, Yao C. Hot cracking in the HAZ of laser-drilled turbine blades made from René 80. *Mater Test* 2005;47:553–9.
- [3] Leigh S, Sezer K, Li L, Grafton-Reed C, Cuttall M. Recast and oxide formation in laser-drilled acute holes in CMSX-4 nickel single-crystal superalloy. *Proc Inst Mech Eng Part B J Eng Manuf* 2010;224:1005–16.
- [4] Chien WT, Hou SC. Investigating the recast layer formed during the laser trepan drilling of Inconel 718 using the Taguchi method. *Int J Adv Manuf Technol* 2007;33:308–16.
- [5] Chen L, Hu WB, Wen ZX, Yue ZF, Gao YF. Effects of roundness of laser formed film cooling holes on fatigue life of nickel based single crystal. *Mater High Temp* 2014;31:18–26.
- [6] Degeilh R, Bonnand V, Pacou D. Study and 3D analysis of the drilling process influence on notched single crystal superalloy specimens. In: *ICMFF9*; 2013.
- [7] Kersey RK, Staroselsky A, Dudzinski DC, Genest M. Thermomechanical fatigue crack growth from laser drilled holes in single crystal nickel based superalloy. *Int J Fatigue* 2013;55:183–93.
- [8] Pan Y, Zimmer R, Bischoff-Beiermann B, Goldschmidt D. Fatigue behaviour of a single crystal nickel superalloy used in heavy-duty gas turbine blade with thin film cooling. *ICF10*, Honolulu, USA; 2001.
- [9] Gemma AE, Phillips JS. The application of fracture mechanics to life prediction of cooling hole configurations in thermal-mechanical fatigue. *Eng Fract Mech* 1977;9:25–36.
- [10] Morar N, Roy R, Mehnen J, Marimuthu S. Investigating recast layer and micro cracks formation during laser trepanning drilling of acute holes in nickel a superalloy. *Cranf Univ*; 2015. p. 1–27. TES 03-15.
- [11] Sengupta A, Putatunda SK, Bartosiewicz L, Hangas J, Nailos PJ, Peputapeck M, et al. Tensile behavior of a new single-crystal nickel-based superalloy (CMSX-4) at room and elevated temperatures. *J Mater Eng Perform* 1994;3:664–72.
- [12] Sun E, Heffernan T, Helmink R. Stress rupture and fatigue in thin wall single crystal superalloys with cooling holes. In: Huron ES, Reed RC, Hardy MC, Mills MJ, Montero RE, Portella PD, et al., editors. *Superalloys 2012*. Hoboken, NJ, USA: John Wiley & Sons, Inc; 2012. p. 353–62.
- [13] Zhou ZJ, Wang L, Wen JL, Lou LH, Zhang J. Effect of skew angle of holes on the tensile behavior of a Ni-base single crystal superalloy. *J Alloys Compd* 2015;628:158–63.
- [14] Pettit F. Hot corrosion of metals and alloys. *Oxid Met* 2011;76:1–21.
- [15] Schneider K, Von Arnim H, Grünling HW. Influence of coatings and hot corrosion on the fatigue behaviour of nickel-based superalloys. *Thin Solid Films* 1981;84:29–36.
- [16] Haight H, Potter A, Sumner J, Gray S. New Technique to Map Hot Corrosion Damage: CMSX-4 Example. *Oxid Met* 2015;84:607–19. <http://dx.doi.org/10.1007/s11085-015-9590-z>.
- [17] Leigh S, Sezer K, Li L, Grafton-Reed C, Cuttall M. Statistical analysis of recast formation in laser drilled acute blind holes in CMSX-4 nickel superalloy. *Int J Adv Manuf Technol* 2009;43:1094–105.
- [18] Sezer HK, Li L, Schmidt M, Pinkerton aj, Anderson B, Williams P. Effect of beam angle on HAZ, recast and oxide layer characteristics in laser drilling of TBC nickel superalloys. *Int J Mach Tools Manuf* 2006;46:1972–82.

# The effect of trepanning speed of laser drilled acute angled cooling holes on the high temperature low cycle corrosion fatigue performance of CMSX-4 at 850°C

Morar, N.

2017-05-04

Attribution 4.0 International

---

Morar N, Roy R, Mehnen J, et al., (2017) The effect of trepanning speed of laser drilled acute angled cooling holes on the high temperature low cycle corrosion fatigue performance of CMSX-4 at 850°C. *International Journal of Fatigue*, Volume 102, September 2017, pp. 112-120

<http://dx.doi.org/10.1016/j.ijfatigue.2017.04.017>

*Downloaded from CERES Research Repository, Cranfield University*